

LAMINAR NATURAL CONVECTION FROM ISOTHERMAL VERTICAL CYLINDERS

Jerod Day

Thesis Prepared for the Degree of

MASTER OF SCIENCE

UNIVERSITY OF NORTH TEXAS

August 2012

APPROVED:

Reza Mirshams, Major Professor
Sandra Boetcher, Committee Member
Matthew Traum, Committee Member
Yong Tao, Chair of the Department of
Mechanical and Energy Engineering
Costas Tsatsoulis, Dean of the College of
Engineering
Mark Wardell, Dean of the Toulouse Graduate
School

Day, Jerod. Laminar natural convection from isothermal vertical cylinders. Master of Science (Mechanical and Energy Engineering), August 2012, 40 pp., 19 figures, 25 numbered references.

Laminar natural convection heat transfer from the vertical surface of a cylinder is a classical subject, which has been studied extensively. Furthermore, this subject has generated some recent interest in the literature. In the present investigation, numerical experiments were performed to determine average Nusselt numbers for isothermal vertical cylinders ($10^3 < Ra_L < 10^9$, $0.5 < L/D < 10$, and $Pr = 0.7$) with and without an adiabatic top in a quiescent ambient environment which will allow for plume growth. Results were compared with commonly used correlations and new average Nusselt number correlations are presented. Furthermore, the limit for which the heat transfer results for a vertical flat plate may be used as an approximation for the heat transfer from a vertical cylinder was investigated.

Copyright 2012

By

Jerod Day

ACKNOWLEDGEMENTS

I would like to thank all the people that contributed to the experiences I have had at the University of North Texas. Good or bad, these experiences have shaped my life and have made me the person I am today.

I owe a great deal to my advisor, Dr. Sandra Boetcher. I can say with great confidence that, without her guidance and encouragement, I would not have been able to maintain my motivation to complete my graduate studies.

Dr. Matthew Traum's thermodynamics class was a welcome escape from the monotonous lectures of most professors. His enthusiasm for teaching and dedication to his students has made him one of the best teacher's I've ever had.

I am grateful for my wife, McKaye, and my son, Kingston, for being there for me through the good and bad times. They have been a great inspiration to me through it all.

TABLE OF CONTENTS

	Page
ACKNOWLEDGEMENTS	iii
LIST OF FIGURES	v
CHAPTER 1 INTRODUCTION	1
1.1 Introduction.....	1
1.2 Nomenclature	1
1.3 Flat Plate Approximation.....	4
1.4 Integral Method.....	4
1.5 Boundary Layer Approximation Method.....	5
1.6 Similarity Solution Method.....	5
1.7 Experiments on Natural Convection from an Isothermal Vertical Cylinder	6
CHAPTER 2 PROBLEM FORMULATION	10
2.1 Physical Model and Solution Domain	10
2.2 Governing Equations	11
2.3 Boundary Conditions	12
2.3.1 Pre-Processing.....	13
2.3.2 Solution.....	14
2.3.3 Post Processing	14
CHAPTER 3 ADIABATIC TOP.....	15
CHAPTER 4 HEATED TOP.....	27
CHAPTER 5 CONCLUSION.....	38
REFERENCES	39

LIST OF FIGURES

	Page
2.1 Solution Domain	10
3.1 Insulated Top Average Nusselt Number versus Rayleigh Number for $AR = 0.1$	15
3.2 Insulated Top Average Nusselt Number versus Rayleigh Number for $AR = 0.125$	16
3.3 Insulated Top Average Nusselt Number versus Rayleigh Number for $AR = 0.2$	17
3.4 Insulated Top Average Nusselt Number versus Rayleigh Number for $AR = 0.5$	18
3.5 Insulated Top Average Nusselt Number versus Rayleigh Number for $AR = 1$	19
3.6 Insulated Top Average Nusselt Number versus Rayleigh Number for $AR = 2$	20
3.7 Insulated Top Average Nusselt Number versus Rayleigh Number for $AR = 5$	21
3.8 Insulated Top Average Nusselt Number versus Rayleigh Number for $AR = 8$	22
3.9 Insulated Top Average Nusselt Number versus Rayleigh Number for $AR = 10$	23
4.1 Comparison of Average Nusselt Number versus Rayleigh Number for $AR = 0.1$	28
4.2 Comparison of Average Nusselt Number versus Rayleigh Number for $AR = 0.125$	29
4.3 Comparison of Average Nusselt Number versus Rayleigh Number for $AR = 0.2$	30
4.4 Comparison of Average Nusselt Number versus Rayleigh Number for $AR = 0.5$	31
4.5 Comparison of Average Nusselt Number versus Rayleigh Number for $AR = 1$	32
4.6 Comparison of Average Nusselt Number versus Rayleigh Number for $AR = 2$	33
4.7 Comparison of Average Nusselt Number versus Rayleigh Number for $AR = 5$	34
4.8 Comparison of Average Nusselt Number versus Rayleigh Number for $AR = 8$	35
4.9 Comparison of Average Nusselt Number versus Rayleigh Number for $AR = 10$	36

CHAPTER 1

INTRODUCTION

1.1 Introduction

Laminar natural convection from isothermal vertical cylinders has its applications in many industries today. One example is the design of vertically oriented electronic pins and components that require cooling from natural convection. Using natural convections as a means of cooling electronic equipment results in a reduced size requirement during design and increases overall efficiency. Equations relating Nusselt number to environmental properties and cylinder size can be found in recent research such as the analysis of the thermo-mechanical behavior of shape memory alloys used in shape memory actuators. [25]

Laminar natural convection heat transfer from the vertical surface of a cylinder is a classical subject, which has been studied extensively. When the boundary layer thickness δ is small compared to the diameter of the cylinder, Nusselt numbers may be determined by approximating the curved vertical surface as a flat plate. However, when the boundary layer thickness is large compared to the diameter of the cylinder, effects of curvature must be taken into account. Many investigators have studied the curvature limits for which the flat-plate model can be applied to estimate Nusselt numbers for vertical cylinders. Furthermore, these investigators have presented Nusselt number correlations for isothermal vertical cylinders.

1.2 Nomenclature

A	coefficient/Area
a	coefficient
AR	aspect ratio, L/D

b	coefficient
BFF	body force function
C	constant
c	coefficient
c_p	specific heat at constant pressure
D	diameter of the cylinder
F	function
f	function
G	function
g	gravitational constant
G_{dyn}	dynamic gravity function
G_{low}	lower-bound gravity function
G_{up}	upper-bound gravity function
$Gr_{\sqrt{A}}$	Grashof number, $g\beta(T_{\text{cylinder}}-T_{\infty})\sqrt{A}^3/\nu^2$
Gr_L	Grashof number, $g\beta(T_{\text{cylinder}}-T_{\infty})L^3/\nu^2$
H	height of solution domain
\bar{h}	average convective heat transfer coefficient
k	thermal conductivity
L	height of cylinder
n	coefficient
$Nu_{\sqrt{A}}$	average Nusselt number, $\bar{h}\sqrt{A}/k$
$Nu_{\sqrt{A}}^0$	conduction limit
Nu_L	average Nusselt number, $\bar{h}L/k$

$Nu_{L,fp}$	average Nusselt number of flat plate
P	dimensionless pressure, $(P-P_{\infty})/\rho(vD)^2$
p	pressure
p_{∞}	free-stream pressure
Pr	Prandtl number, $c_p\mu/k$
R,Z	dimensionless cylindrical coordinates, $(r,z)/D$
r,z	cylindrical coordinates
Ra_L	Rayleigh number, Gr_LPr
T	temperature
$T_{cylinder}$	temperature at the vertical surface of the cylinder
T_{∞}	temperature of the ambient environment
U_R, U_Z	dimensionless velocity components, $(u_r, u_z)/(v/D)$
W	width of solution domain

Greek

β	isobaric coefficient of thermal expansion
δ	boundary layer thickness
θ	dimensionless temperature, $(T-T_{\infty})/(T_{cylinder}-T_{\infty})$
μ	dynamic viscosity of the fluid
ν	kinematic viscosity of the fluid
ξ	curvature parameter, $(4L/D)(Gr_L/4)^{-1/4}$
ρ	density of the fluid

1.3 Flat Plate Approximation

In most heat transfer textbooks, including but not limited to Incropera et al. [1, 2], Holman [3], Burmeister [4], and Gebhart et al. [5], the accepted limit for which the flat-plate solution can be used to approximate average Nusselt numbers for vertical cylinders ($Pr = 0.72$) within 5% error is

$$\frac{D}{L} \geq \frac{35}{Gr_L^{0.25}} \quad (1.1)$$

where D is the diameter of the cylinder, L is the height of the cylinder, and Gr_L is the Grashof number based on the height of the cylinder. This limit was derived by Sparrow and Gregg [6] in 1956 using a pseudo-similarity variable coordinate transformation and perturbation technique for solving the heat transfer and fluid flow adjacent to an isothermal vertical cylinder. They assumed the boundary layer thickness at the leading edge to be zero and they made use of the boundary layer approximation (all pressure gradients are zero and streamwise second derivatives are neglected) and Boussinesq approximation (density difference are small). In addition, Nusselt numbers for vertical cylinders ($Pr = 0.72$ and 1 ; $0 < \xi < 1$) are presented as a truncated series solution and plotted. The curvature parameter ξ arose from a coordinate transformation done by [6] and is defined as

$$\xi = \frac{4L}{D} \left(\frac{Gr_L}{4} \right)^{-1/4} \quad (1.2)$$

1.4 Integral Method

Around the same time as Sparrow and Gregg, Le Fevre and Ede [7, 8] solved the governing equations using the same assumptions as [6] with an integral method to obtain a correlation for vertical cylinder average Nusselt numbers, which is shown below.

$$Nu_L = \frac{4}{3} \left[\frac{7Gr_L Pr}{5(20+21Pr)} \right] + \frac{4(272+315Pr)L}{35(64+63Pr)D} \quad (1.3)$$

In this equation, Nu_L is the average Nusselt number and Pr is the Prandtl number.

1.5 Boundary Layer Approximation Method

In 1974, Cebeci [9] extended the work of [6] by numerically solving the governing equations using the boundary-layer approximation for $0.01 \leq Pr \leq 100$ and $0 < \xi < 5$. The results of Cebeci for the average Nusselt number for an isothermal vertical cylinder $Pr = 0.72$ have been correlated in Popiel [10] with range of deviation from -0.34% - 0.66%

$$\frac{Nu_L}{Nu_{L,fp}} = 1 + 0.3 \left[32^{0.5} Gr_L^{-0.25} \frac{L}{D} \right]^{0.909} \quad (1.4)$$

In this equation, $Nu_{L,fp}$ is the average Nusselt number for the isothermal flat plate.

Typically, the value for $Nu_{L,fp}$ is taken from the Churchill and Chu [11] correlations for natural convection from a vertical flat plate.

$$Nu_{L,fp} = 0.68 + \frac{0.670 Ra_L^{1/4}}{[1 + (0.492/Pr)^{9/16}]^{4/9}} \quad (1.5)$$

In this equation, Ra_L is the Rayleigh number based on the height of the cylinder. Also in 1974, Minkowycz and Sparrow [12] continued the work of [6] by investigating the impact of different levels of truncation in the series solution. Their findings indicate good agreement with [6] with a maximum deviation of 4% between the average Nusselt number solutions. They obtained results in graphical form for $0 < \xi < 10$ and for $Pr = 0.733$.

1.6 Similarity Solution Method

In the late 1980s, Lee et al. [13] solved the boundary layer equations for non-uniform wall temperature using the similarity solution method. Their work extends that of Fujii and

Uehara [14], except that unlike the authors of [14] who present information for local Nusselt numbers only, the authors of [13] present correlations for both the local and average Nusselt numbers for $0 < \xi < 70$. The average Nusselt number correlation in [13] for $0.1 \leq \text{Pr} \leq 100$ when the wall temperature is uniform is reduced to

$$\ln \left[\text{Nu}_L \left(\frac{\text{Gr}_L}{4} \right)^{-1/4} \right] = F(\xi) + \left\{ \ln \left[\text{Nu}_{L,\text{fp}} \left(\frac{\text{Gr}_L}{4} \right)^{-1/4} + 2.92629 \right] \right\} \exp(-G\xi^{1/2}) \quad (1.6)$$

and F and G are functions such that

$$F(\xi) = -2.92620 + 1.66850\xi^{1/2} - 0.21909\xi + 0.011308\xi^{3/2} \quad (1.7)$$

and

$$G = 0.29369 + 0.3263\text{Pr}^{-0.19305} \quad (1.8)$$

with $\text{Nu}_{L,\text{fp}}$ being defined as

$$\text{Nu}_{L,\text{fp}} \left(\frac{\text{Gr}_L}{4} \right)^{-1/4} = (2\text{Pr})^{1/2} [2.5(1 + 2\text{Pr}^{1/2} + 2\text{Pr})]^{-1/4} \quad (1.9)$$

1.7 Experiments on Natural Convection from an Isothermal Vertical Cylinder

Although much classical work on the natural convection heat transfer from isothermal vertical cylinders has been reported, there has been recent interest in the subject as seen by a contemporary review article in 2008 on the subject by Popiel [10]. In 2003, Muñoz-Cobo et al. [15] studied power-law temperature distributions following on the work of Lee et al. [13]. In addition, several investigators have recently used either experimental means [16, 17] or older analytical and numerical techniques [18] to study natural convection from a vertical cylinder.

Popiel et al. [17] conducted an experimental study on natural convection from an isothermal vertical cylinder. The investigators in [17], using the data reported in [9], propose a

new limit for which the flat plate solution can be used to approximate the average Nusselt numbers with 3% error

$$Gr_L^{0.25} \frac{D}{L} \leq a + \frac{b}{Pr^{0.5}} + \frac{c}{Pr^2} \quad (1.10)$$

where $a = 11.474$, $b = 48.92$, and $c = -0.0006085$. Furthermore, experiments were conducted on an isothermal vertical cylinder with an insulated top situated on an insulated surface for $Pr = 0.71$, $1.5 \times 10^8 < Ra_L < 1.1 \times 10^9$, and $0 < L/D < 60$. The results of this study were correlated into the following equation

$$Nu_L \leq A Ra_L^n \quad (1.11)$$

where

$$A = 0.519 + 0.03454 \frac{L}{D} + 0.0008772 \left(\frac{L}{D} \right)^2 + 8.855 \times 10^{-6} \left(\frac{L}{D} \right)^3 \quad (1.12)$$

and

$$n = 0.25 - 0.00253 \frac{L}{D} + 1.152 \times 10^{-5} \left(\frac{L}{D} \right)^2 \quad (1.13)$$

Their results agree fairly well with Cebeci [9] for the higher Rayleigh numbers which were studied.

In the majority of the work done on natural convection heat transfer from vertical cylinders, the top of the cylinder is usually assumed to be adiabatic. Despite the vast amounts of literature available, to the best knowledge of the authors, very few investigators have studied the effect of a heated top on the average Nusselt number. In 1978, Oosthuizen [19] examined the effect of cylinders having heated exposed ends on the average Nusselt number. In general, he found that the average Nusselt numbers for the heated ends was up to 30% lower in some cases compared to the equivalent cylinder with an adiabatic end.

Very recently, Eslami and Jafarpur [20] (who built upon the previous work of several other studies [21–24]) investigated laminar natural convection from isothermal cylinders with active ends. These authors present a generalized semi-empirical method to calculate average Nusselt numbers from arbitrary shapes in which they use to present results for specific geometric cases, including vertical cylinders. The generalized equation for the Nusselt number for a vertical cylinder with one active end (heated top) based on the square-root of the area is

$$Nu_{\sqrt{A}} = Nu_{\sqrt{A}}^0 + f(Pr) G_{\text{dyn}} Ra_{\sqrt{A}}^{1/4} \quad (1.14)$$

where $f(Pr)$ is the Prandtl function

$$f(Pr) = \frac{0.670}{[1 + (0.5/Pr)^{9/16}]^{4/9}} \quad (1.15)$$

and the dynamic gravity function is defined as

$$G_{\text{dyn}} = \frac{BFF + \frac{G_{\text{up}}}{G_{\text{low}}} Ra_{\sqrt{A}}^{1/4}}{BFF + C \cdot Ra_{\sqrt{A}}^{1/4}} C \cdot G_{\text{low}} \quad (1.15)$$

where the body force function is

$$BFF = \frac{Nu_{\sqrt{A}}^0}{f(Pr) G_{\text{low}}} \quad (1.16)$$

$$C = 0.34 + 0.046 \cdot BFF \quad (1.17)$$

and the lower-bound and upper-bound gravity force functions specifically for a vertical cylinder with one heated end are

$$G_{\text{low}} = \left[0.952^{4/3} \left(\frac{\pi D^2/4}{\pi D^2/4 + \pi DL} \right)^{7/6} + [1.154(D/L)^{1/8}]^{4/3} \left(\frac{\pi DL}{\pi D^2/4 + \pi DL} \right)^{7/6} \right]^{3/4} \quad (1.18)$$

$$G_{\text{up}} = 0.952 \left(\frac{\pi D^2/4}{\pi D^2/4 + \pi DL} \right)^{7/8} + 1.154(D/L)^{1/8} \left(\frac{\pi DL}{\pi D^2/4 + \pi DL} \right)^{7/8} \quad (1.19)$$

The conduction limit for circular cylinders $0 \leq L/D \leq 8$ is

$$Nu_{\sqrt{A}}^0 = \frac{8.00 + 6.95(L/D)^{0.76}}{[2\pi + 4\pi(L/D)]^{1/2}} \quad (1.20)$$

The Nusselt numbers based on the square-root of the area were converted to Nusselt numbers based on the height (L) of the cylinders when later compared to the results of the present study.

High-quality natural convection heat transfer experiments that correctly interrogate heated shapes in air are inherently difficult to perform, which is reflected in the lack of experimental data available in the literature. Much analytical and numerical work is inconsistent due to the practices of 1) neglecting the streamwise second derivative in the Navier-Stokes equation (i.e., using boundary-layer approximation), 2) using boundary conditions that are not representative of the space surrounding real objects, and 3) method of solution (integral, pseudo-similarity, finite-difference). Previous work typically places the boundary at the top of the cylinder instead of considering the effect of the resulting plume on the boundary layer of the vertical surface. In addition, the majority of previous investigators ignored the effect of a heated top in the calculation of the average Nusselt numbers.

The goal of this work is to perform numerical experiments which take into account the streamwise second derivatives in the governing equations and allow for full plume growth to determine average Nusselt numbers for laminar isothermal vertical cylinders ($10^2 < Ra_L < 10^9$, $0.1 < L/D < 10$, and $Pr = 0.7$) situated on an adiabatic surface in a quiescent ambient environment which will allow for plume growth. The results will be compared against all other known classical solutions for isothermal vertical cylinders. Furthermore, the validity of Eqs. (1) and (10) for determining the range at which the flat-plate solution may be used as an approximation for a vertical cylinder will be investigated. Lastly, the effect of ignoring a heated top on the average Nusselt numbers will be shown.

CHAPTER 2

PROBLEM FORMULATION

2.1 Physical Model and Solution Domain

Consider a vertical cylinder with isothermal walls and an adiabatic or heated top of diameter D and height L situated on an adiabatic surface in a quiescent, constant-temperature ambient environment. The top will either be adiabatic in order to investigate the accuracy of the classical side-wall solutions, or isothermal (heated top) in order to compare against the adiabatic-top case. Due to both geometric and thermal axisymmetry, this problem may be modeled as two-dimensional.

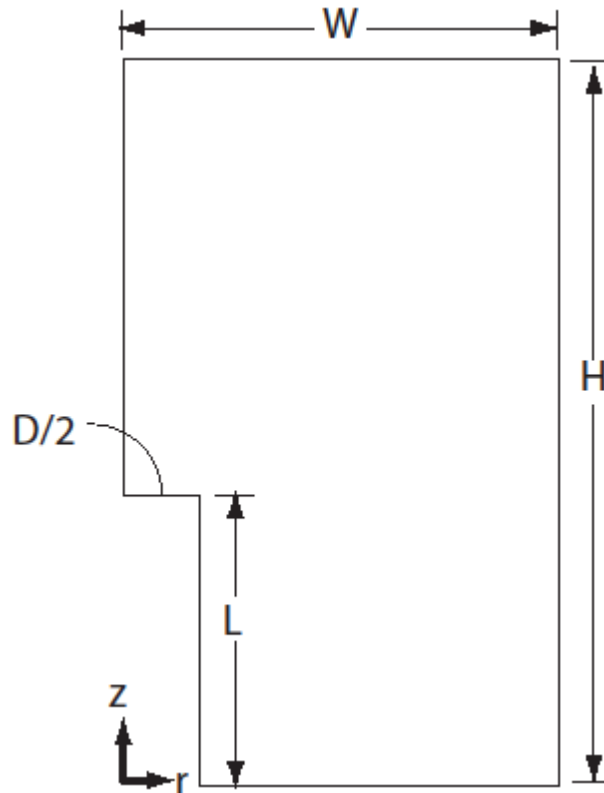


Fig. 2.1 Solution Domain

In Fig. 2.1 r and z are the radial and axial coordinates, respectively. Furthermore, W is the width of the solution domain which is set to $5D$ and H is the height of the solution domain

which is equal to $(24D + L)$. The aspect ratio of the cylinder, $AR=L/D$, is varied parametrically, $0.1 \leq AR \leq 10$.

2.2 Governing Equations

The subsequent dimensionless variables are used in writing the governing equations

$$R = \frac{r}{L}, Z = \frac{z}{L}, U_R = \frac{u_r}{(v/L)}, U_Z = \frac{u_z}{(v/L)}, P = \frac{p-p_\infty}{\rho(v/L)^2}, \theta = \frac{T-T_\infty}{T_{cylinder}-T_\infty} \quad (2.1)$$

and

$$Gr_L = \frac{g\beta(T_w-T_\infty)L^3}{\nu^2}, Pr = \frac{c_p\mu}{k} \quad (2.2)$$

Here, r and z are the radial and axial coordinates respectively, u_r and u_z are the radial and axial velocity components, ν is the kinematic viscosity, T is the temperature, $T_{cylinder}$ is the temperature at the wall of the cylinder, T_∞ is the ambient temperature far from the cylinder, p is the local pressure, p_∞ is the freestream pressure, g is gravity, β is the coefficient of thermal expansion, c_p is the specific heat at constant pressure, μ is the dynamic viscosity and k is the thermal conductivity. All thermal properties are assumed to be constant.

The governing equations for axisymmetric, laminar, incompressible, natural convection flow are

- Conservation of mass

$$\frac{1}{R} \frac{\partial(RU_R)}{\partial R} + \frac{\partial(U_Z)}{\partial Z} = 0 \quad (2.3)$$

- Conservation of momentum in the Z-direction

$$U_R \frac{\partial U_Z}{\partial R} + U_Z \frac{\partial U_Z}{\partial Z} = -\frac{\partial P}{\partial Z} + \frac{1}{R} \frac{\partial}{\partial R} \left(R \frac{\partial U_Z}{\partial R} \right) + \frac{\partial^2 U_Z}{\partial Z^2} + Gr_L \theta \quad (2.4)$$

- Conservation of momentum in the R-direction

$$U_R \frac{\partial U_R}{\partial R} + U_Z \frac{\partial U_R}{\partial Z} = -\frac{\partial P}{\partial R} + \frac{1}{R} \frac{\partial}{\partial R} \left(R \frac{\partial U_R}{\partial R} \right) + \frac{\partial^2 U_R}{\partial Z^2} - \frac{U_R}{R^2} \quad (2.5)$$

- Conservation of energy

$$U_R \frac{\partial \theta}{\partial R} + U_Z \frac{\partial \theta}{\partial Z} = \frac{1}{Pr} \left[\frac{1}{R} \frac{\partial}{\partial R} \left(R \frac{\partial \theta}{\partial R} \right) + \frac{\partial^2 \theta}{\partial Z^2} \right] \quad (2.6)$$

The Boussinesq approximation can be employed here due to negligible density differences. The viscous dissipation and work terms can be neglected in the energy equation because of the small velocities encountered in natural convection flow.

2.3 Boundary Conditions

The temperature at the vertical surface of the cylinder is T_{cylinder} and the no-slip condition is applied. The boundary conditions at the surface of the cylinder in dimensionless form are

$$U_Z = U_R = 0 \text{ and } \theta = 1 \quad (2.7)$$

The top surface of the cylinder is either adiabatic

$$\frac{\partial \theta}{\partial Z} = 0 \quad (2.8)$$

or isothermal

$$\theta = 1 \quad (2.9)$$

In both cases, no-slip applies

$$U_Z = U_R = 0 \quad (2.10)$$

On the bottom surface of the fluid domain, adiabatic and no-slip boundary conditions are applied such that

$$U_Z = U_R = 0 \text{ and } \frac{\partial \theta}{\partial Z} = 0 \quad (2.11)$$

Along the axis of symmetry ($R = 0$) the boundary conditions are

$$U_R = \frac{\partial U_Z}{\partial R} = \frac{\partial \theta}{\partial R} = 0 \quad (2.12)$$

Relatively weak boundary conditions (the so-called opening condition in ANSYS CFX) are placed at the far-field boundaries at the top and side of the solution domain. The conditions allow the flow to either entrain into the domain or flow out. Specified at these boundaries are the pressure and the temperature of the fluid if entering into the domain.

At the top of the solution domain

$$P=0 \text{ and } \theta=0 \text{ if } U_Z < 0 \quad (2.13)$$

Along the side of the solution domain

$$P=0 \text{ and } \theta=0 \text{ if } U_R < 0 \quad (2.14)$$

2.3.1 Pre-Processing

The solution geometries, blocking, and meshes were created using ANSYS ICEM CFD 11.0. Due to the geometric and thermal axisymmetry and the need to minimize computational resources, the geometries consist of a 1° section of the total solution domain.

In order to create a hexahedral mesh, the curves of the geometry must be associated to the edges of blocks using a method known as blocking. The surfaces formed by these edges were given common names to aid in identifying fluid boundaries during pre-processing. The edges of these blocks were then divided into hexahedral mesh volumes concentrating the most nodes in the areas of interest. A hexahedral unstructured mesh is outputted using the parameters defined in the block file.

ANSYS CFX-Pre is the physics-definition pre-processor for ANSYS CFX. The hexahedral unstructured mesh file is imported into ANSYS CFX-Pre in order to define the fluid

properties, flow characteristics, and boundary conditions. Once all properties and boundary conditions have been defined, a definition file containing all the necessary information to run the simulation is outputted.

2.3.2 Solution

ANSYS CFX 12.0, a finite-volume-based computational fluid dynamics solver, was used to perform the numerical experiments. Unlike the classical methods of using the integral method, solving for the boundary layer equations, using semi-empirical analysis, and/or perturbation techniques, ANSYS CFX 12.0 solves for the full conservation of mass, momentum, and energy equations. Furthermore, in the numerical approach here, solution domain boundaries are extended further out minimizing boundary condition assumptions in the area of the flow (i.e. the plume at the top of the cylinder is allowed to grow, whereas in the classical solutions, the boundary is cut-off at the top of the cylinder).

The number of nodes used was 210,000. Mesh independence was established by multiplying the number of nodes by two. The average Nusselt numbers of the two meshes varied by less than 0.3%. The boundaries of the solution domain were placed far enough away as to not affect the solution of the area of interest, in this case, the heat transfer at the cylinder. In addition, the height and width of the solution domain were varied and tested.

2.3.3 Post Processing

The result files of the simulations were analyzed in ANSYS CFX-Post. Using the ANSYS CFX-Post Function Calculator, average wall heat flux values were extracted from the surfaces of the cylinder in order to calculate the average convective heat transfer coefficient, \bar{h} . With an average convective heat transfer coefficient, the Nusselt number, Nu_L , can be calculated.

CHAPTER 3

ADIABATIC TOP

Results will now be presented to compare the current work to other classical solutions for laminar natural convection from an isothermal cylinder with an adiabatic top.

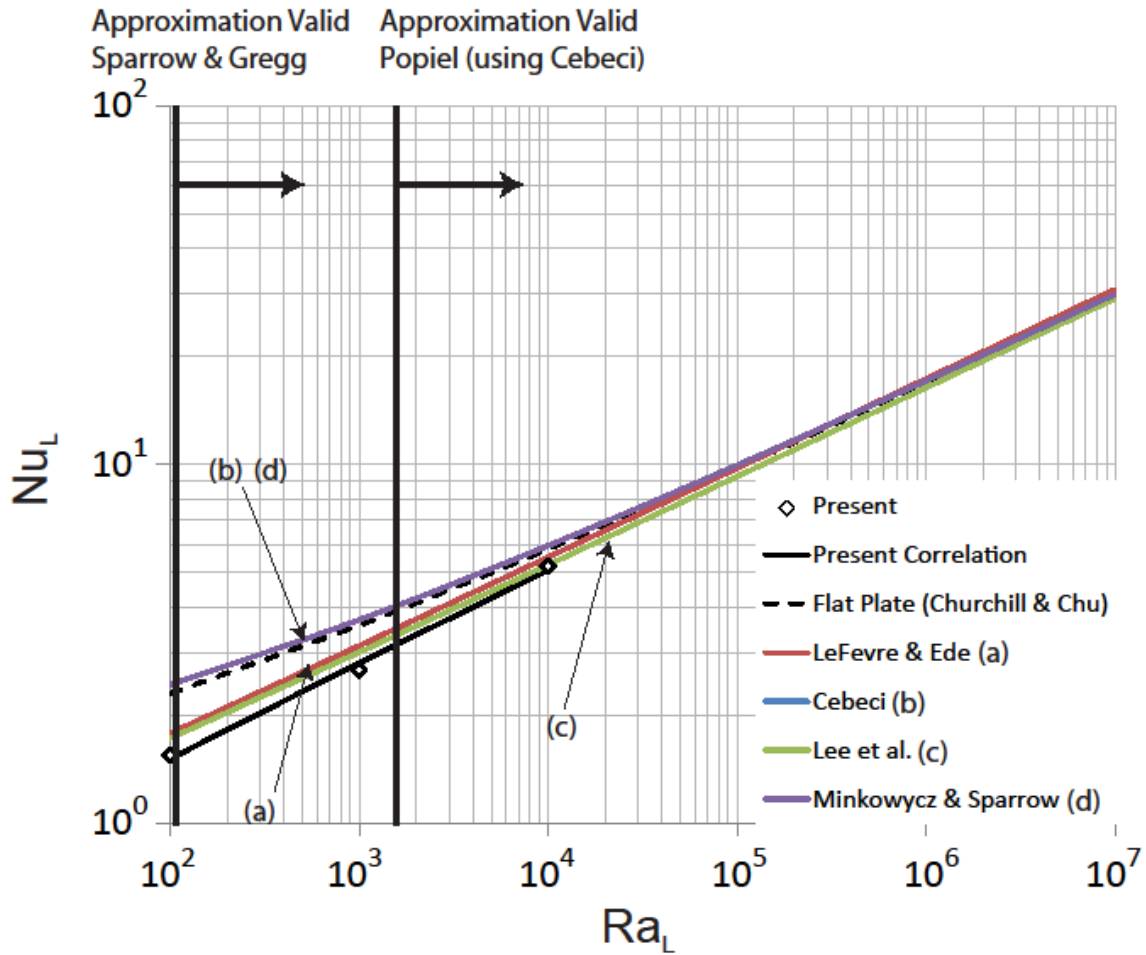


Fig. 3.1 Insulated Top Average Nusselt Number versus Rayleigh Number for $AR = 0.1$.

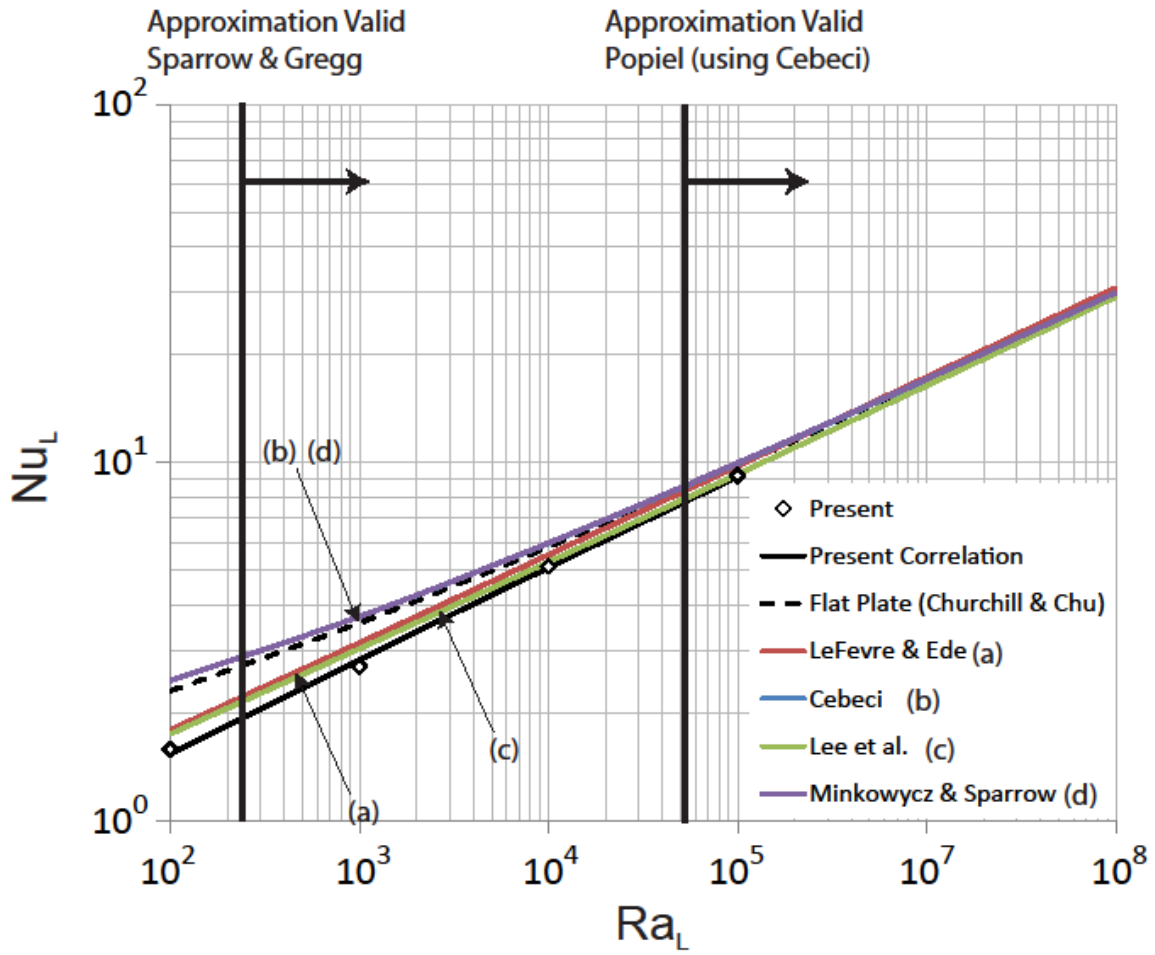


Fig. 3.2 Insulated Top Average Nusselt Number versus Rayleigh Number for $AR = 0.125$.

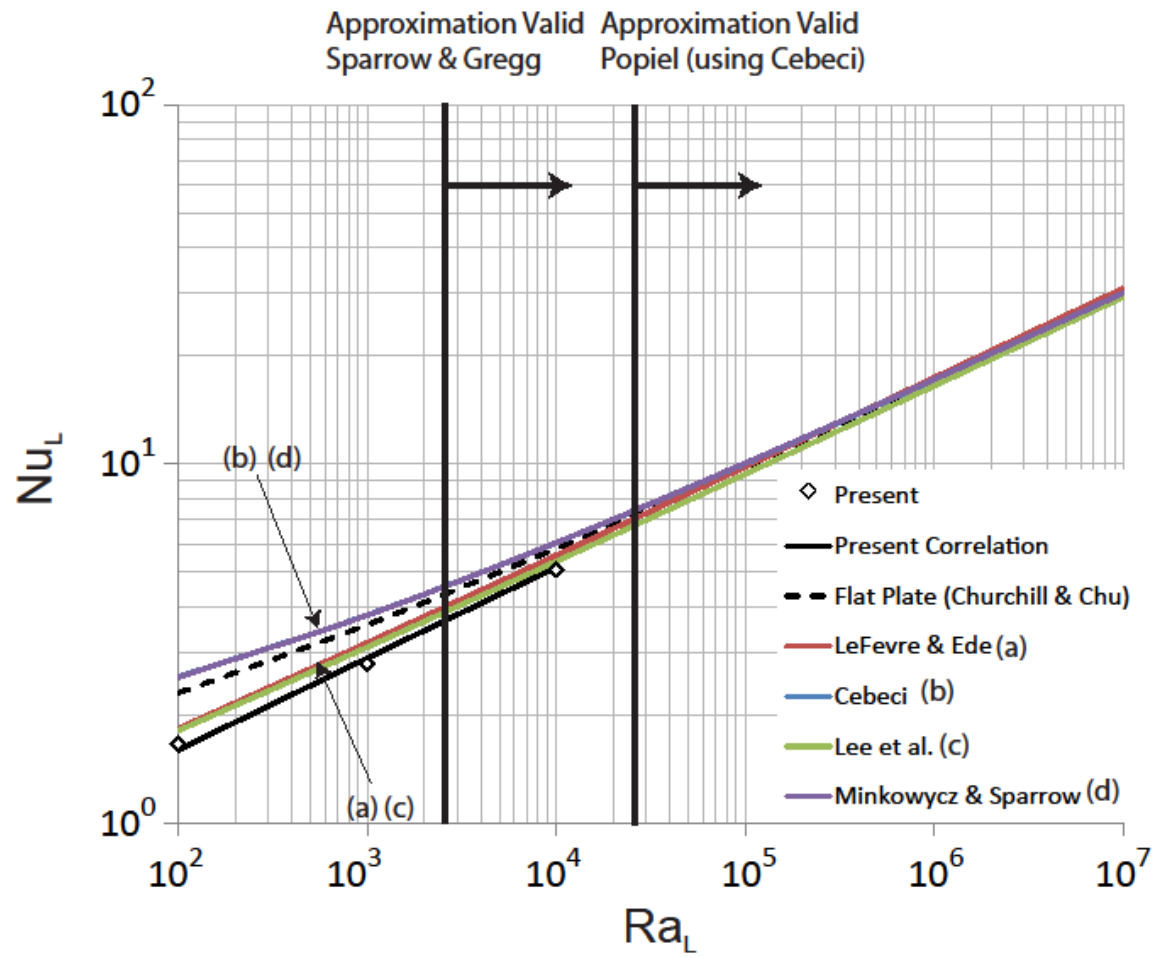


Fig. 3.3 Insulated Top Average Nusselt Number versus Rayleigh Number for $AR = 0.2$.

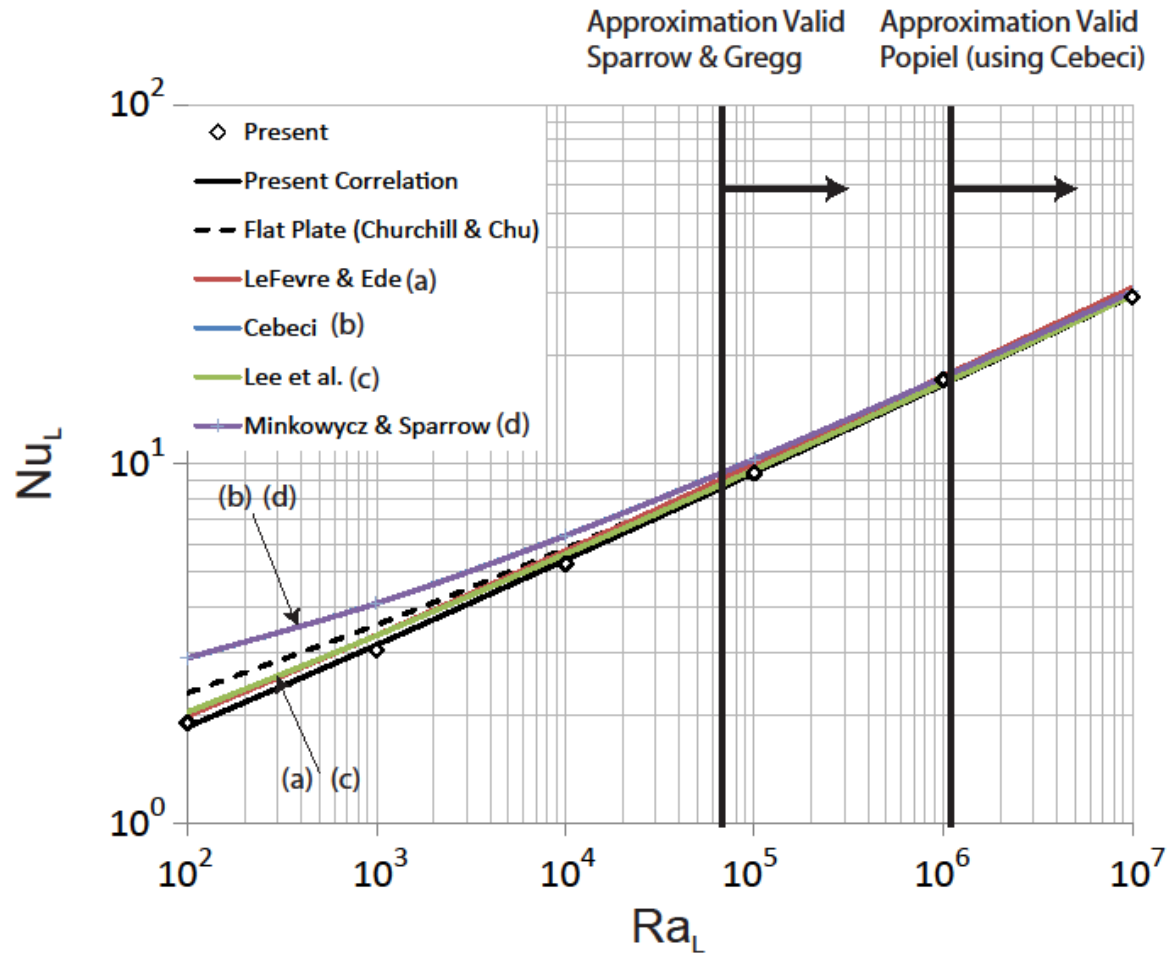


Fig. 3.4 Insulated Top Average Nusselt Number versus Rayleigh Number for $AR = 0.5$.

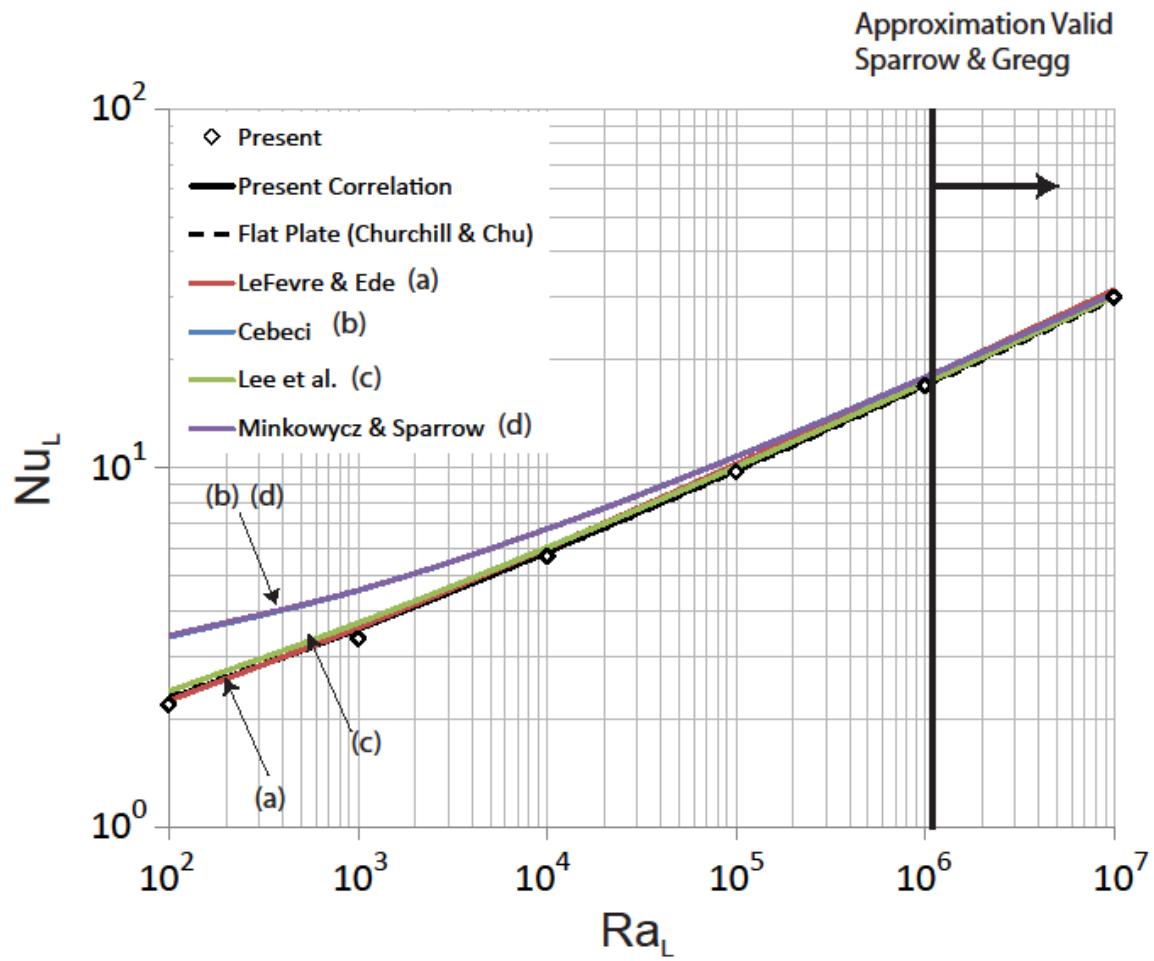


Fig. 3.5 Insulated Top Average Nusselt Number versus Rayleigh Number for $AR = 1$.

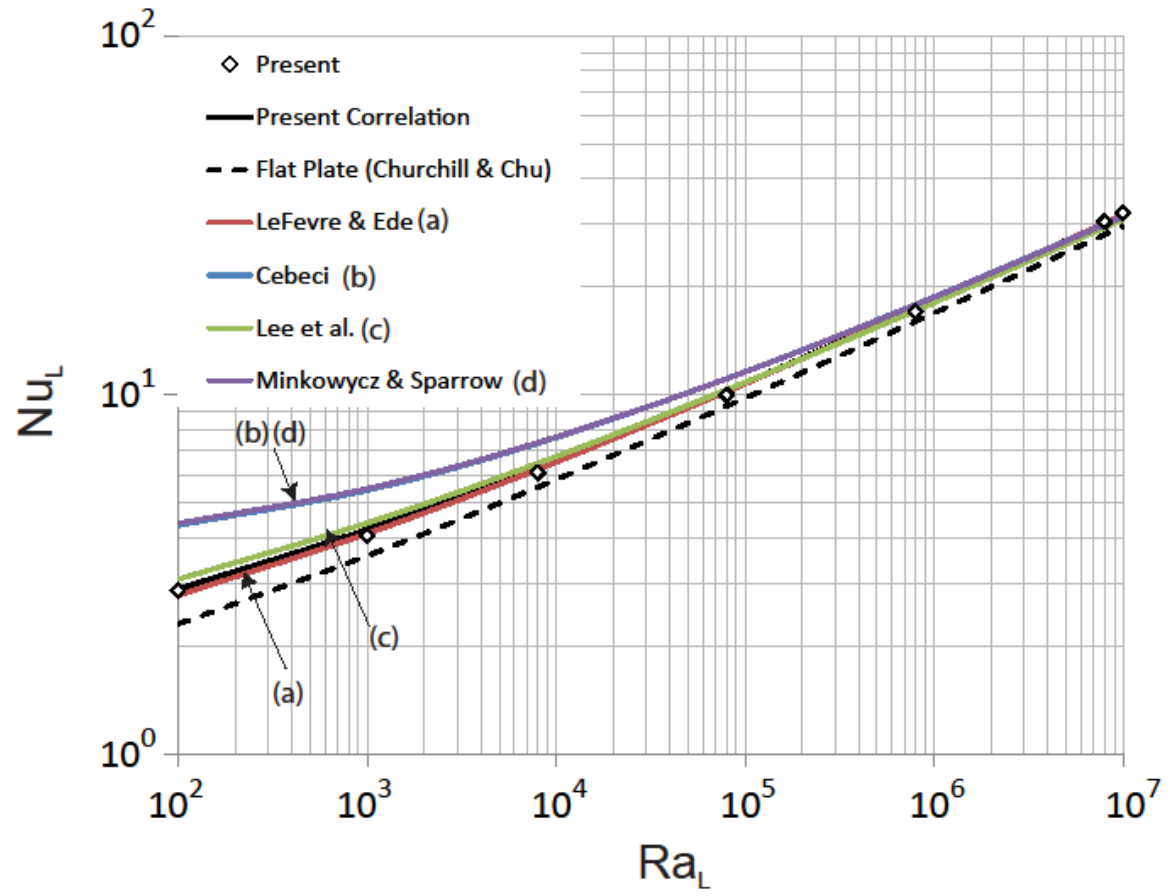


Fig. 3.6 Insulated Top Average Nusselt Number versus Rayleigh Number for $AR = 2$.

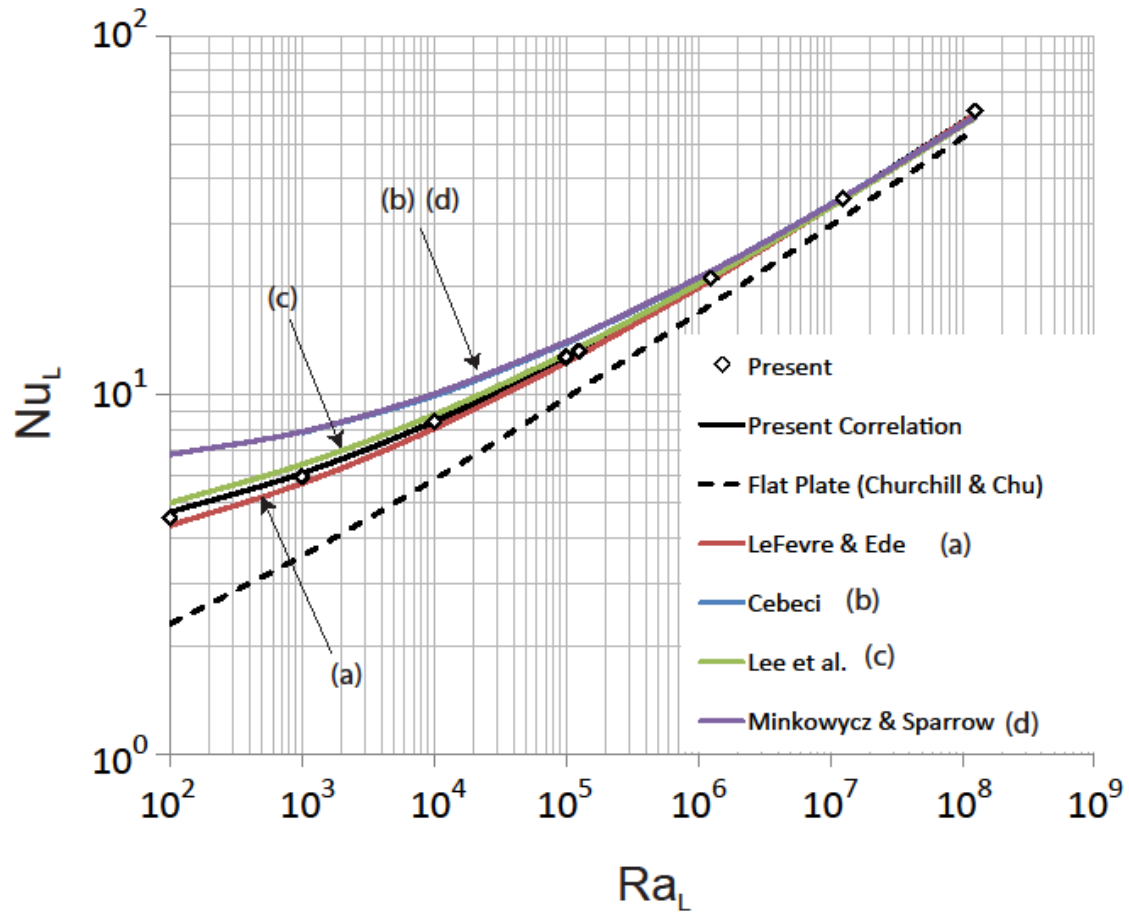


Fig. 3.7 Insulated Top Average Nusselt Number versus Rayleigh Number for $AR = 5$.

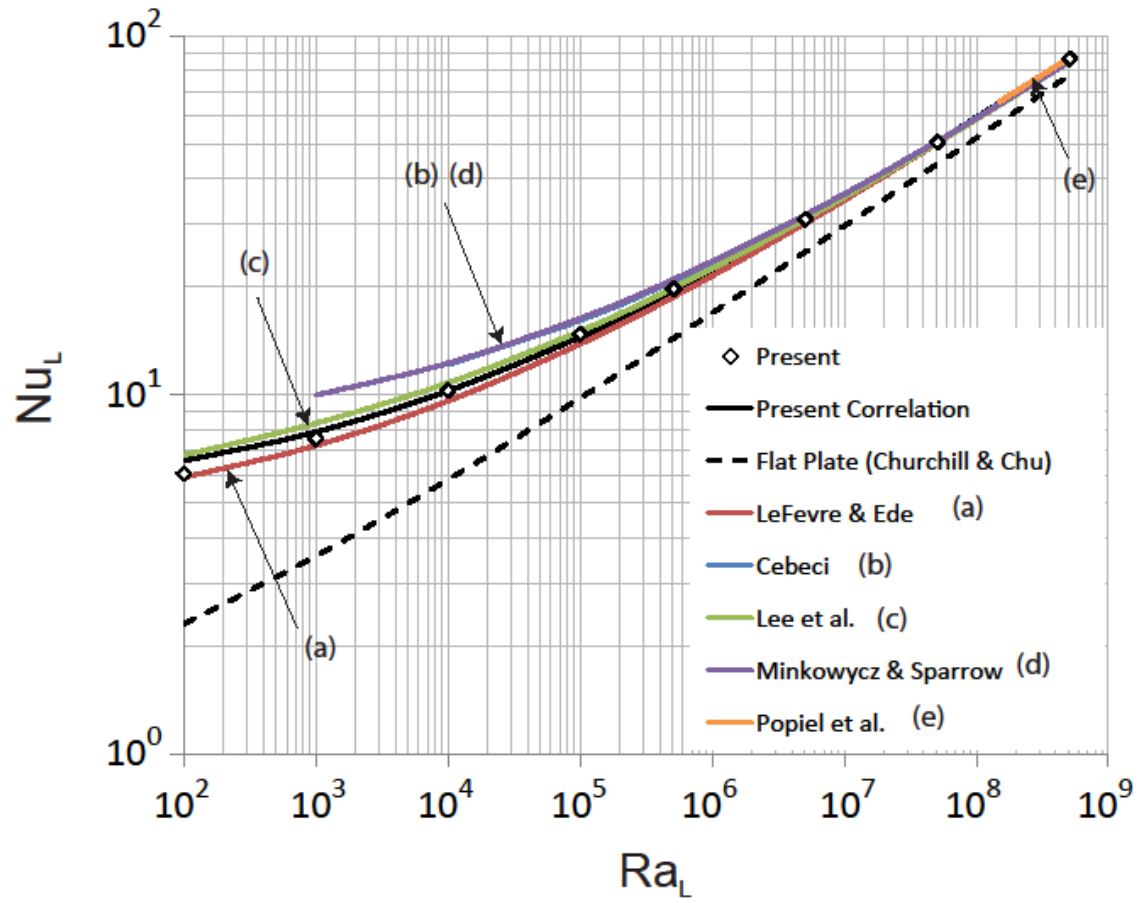


Fig. 3.8 Insulated Top Average Nusselt Number versus Rayleigh Number for $AR = 8$.

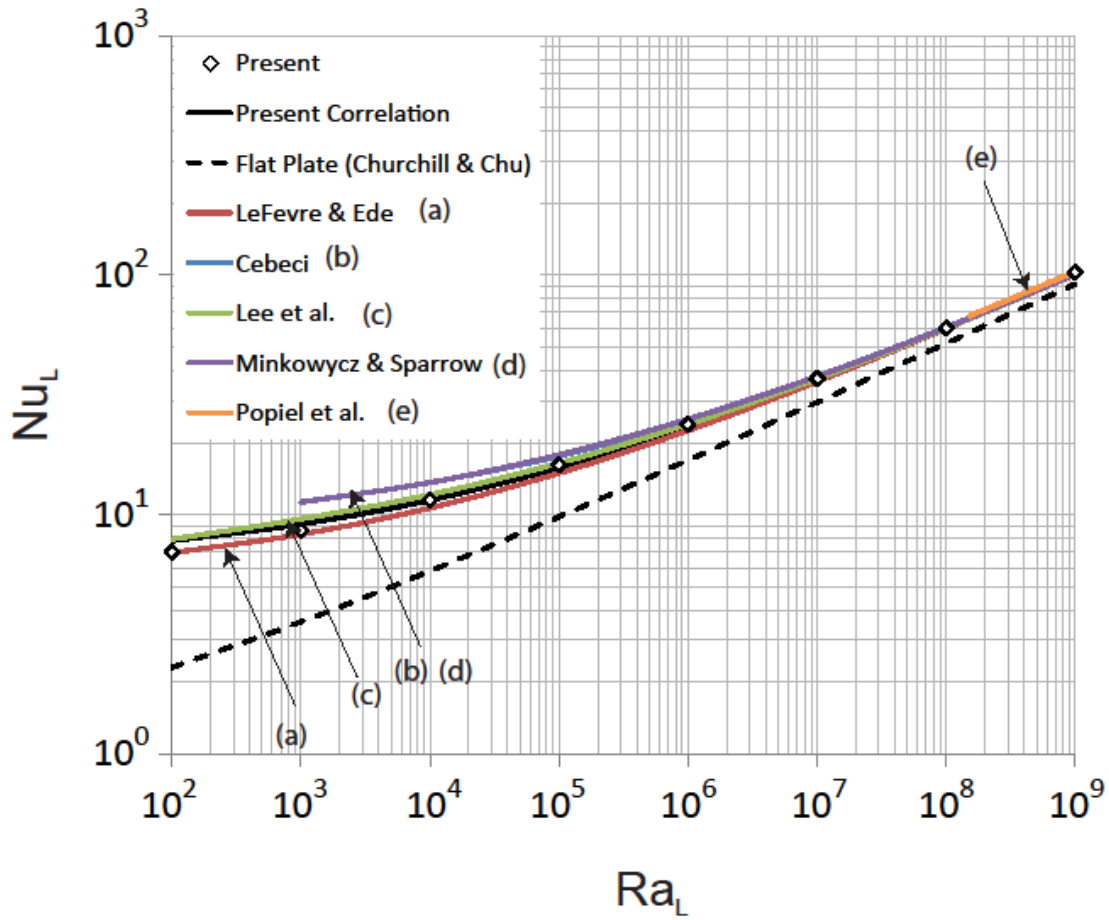


Fig. 3.9 Insulated Top Average Nusselt Number versus Rayleigh Number for $AR = 10$.

Figures 3.1-3.9 have been prepared to show the average Nusselt numbers versus Rayleigh number for several different aspect ratios. The current numerical experiments (Present) are compared with previous work by LeFevre and Ede [7, 8] -Eq. (1.3), Cebeci [9] - Eq. (1.4), Minkowycz and Sparrow [12], Lee et al. [13] - Eqs. (1.6-1.9), Popiel [10] - Eqs. (1.10-1.13), and the isothermal laminar vertical flat plate correlation from Churchill and Chu [11] - Eq. (1.5). Furthermore, the present data has been correlated into an equations for $Pr = 0.7$ and plotted in the figures. The resulting correlation was developed using the MATLAB surface fitting tool using a

non-linear least squares method with a LAR robust algorithm and are presented below. The R-squared value was 0.9999.

For $0.1 \leq AR \leq 1$

$$Nu_L = -0.2165 + 0.5204 Ra_L^{1/4} + 0.8473 \left(\frac{L}{D} \right) \quad (3.1)$$

For $2 \leq AR \leq 10$

$$Nu_L = -0.06211 + 0.54414 Ra_L^{1/4} + 0.6123 \left(\frac{L}{D} \right) \quad (3.2)$$

The applicability limits of vertical flat-plate solution as an approximation of the average heat transfer coefficient for an isothermal vertical cylinder are shown in Figs. 2 - 6 by solid vertical black line (for Figs. 7 - 10 the limits are located at Ra_L greater than those of interest). These figures include the range proposed by Sparrow and Gregg [6] (Eq. 1.1)) (within 5% of flat-plate) and the more conservative estimate provided by Popiel using the data of Cebeci [9, 10] (Eq. 1.10)) (within 3% of flat-plate) .

As the Rayleigh number increases, all solutions asymptotically approach the flat-plate solution. As the aspect ratio increases, the cut-off Rayleigh number for which the flat-plate solution can be used to approximate the Nusselt number increases.

For $AR = 0.1$, Sparrow and Gregg claim that the flat-plate solution can be used to approximate Nusselt numbers for Ra_L greater than 100. However, upon inspection of Fig. 2, the present solution deviates from that of the flat plate by as much as 32%. Furthermore, the present solution deviates from that of Minkowycz and Sparrow (virtually the exact same results as Cebeci) by upwards of 36%. It is interesting to note, that the solutions of LeFevre and Ede were determined using an integral method, yet the deviation from that solution and the present solution is approximately 13%. Furthermore, the solutions of Lee et al. are very close to that of

LeFevre and Ede. Extrapolation of results for $AR = 0.1$ places the limit at $Ra_L \approx 10^5$ for 5% deviation from the flat plate.

Figures 3 - 6 present similar stories. The present data is closer to that of LeFevre and Ede than it is to Minkowycz and Sparrow (Cebeci); and the higher the aspect ratio, the closer the present solution is to LeFevre and Ede. Also observed is that the higher the aspect ratio, the closer the present solution (and LeFevre and Ede) approaches that of the flat-plate solution in this range of aspect ratios ($0.1 \leq AR \leq 1$). Interestingly, the reverse trend is seen in the data of Minkowycz and Sparrow (Cebeci)- as the aspect ratio increases, the data gets farther away from the flat-plate solution, which is evidenced by the approximation line increasing in Rayleigh number. At one end of the spectrum, $AR = 0.1$, the Sparrow and Gregg limit is too liberal (and not accurate) in predicting when to use the flat-plate solution to approximate the heat transfer from the curved side, and when $AR = 1$, the Sparrow and Gregg limit is far too conservative in determining when to the flat-plate solution is appropriate.

For $AR = 0.125$, the limit placed at $Ra_L \approx 10^5$ for 6% deviation from the flat plate. Extrapolating, for $AR = 0.2$, Nusselt numbers deviate approximately 5% at $Ra_L \approx 10^5$. For $AR = 0.5$ and $AR = 1$, the limit can be placed at $Ra_L \approx 10^5$ and $Ra_L \approx 10^3$ for 4% and 6% deviations, respectively.

Next, attention will be turned to Figs. 7 - 10. In this group of aspect ratios (which are representing more tall, slender cylinders: $2 \leq AR \leq 10$), there is no question that any of the solutions can be approximated using the flat plate. Here, the results of LeFevre and Ede and Lee et al. differ slightly more, with the present solution found in between these two. For $AR = 2$, the present results differ from Minkowycz and Sparrow (Cebeci) by as much as 34%. As the aspect ratios increase, the percent difference between all of the solutions decreases. As an aside, for AR

= 8 and 10, the lower Rayleigh numbers are out of the range of curvature parameters for which the Minkowycz and Sparrow (Cebeci) solutions are valid ($0 < \xi < 10$) and are therefore not plotted.

It is of particular interest to note that in many heat transfer textbooks, including [1–3], after being instructed to determine whether curvature effects are important using Eq. (1.1), the reader is directed to use the results of [6], [9], and/or [12], which are the results from Sparrow and Minkowycz and Cebeci.

CHAPTER 4

HEATED TOP

As was mentioned in the Chapter 1, very little work has been presented on natural convection from vertical cylinders with heated tops. Oosthuizen [19] included in his work the case of an isothermal cylinder situated upright on an adiabatic base with a heated top (like the present). Oosthuizen's experimental data includes only 11 data points, two of which fall under the same aspect ratios simulated here $AR = 1$ and 2 . Eslami and Jafarpur [20] presented the case of an isothermal cylinder with both ends (top and bottom) active. The current authors used the generalized equations presented in [20] to determine the average Nusselt numbers for an isothermal cylinder with only the side and top heated and have included this data with the present results (details in the Chapter 1).

Similar to the adiabatic case, the present data was correlated using the same method and plotted using the following equations.

For $0.1 \leq AR \leq 0.2$

$$Nu_L = -0.2823 + 0.2657 Ra_L^{1/4} + 3.657 \left(\frac{L}{D} \right) \quad (4.1)$$

For $AR = 0.5$

$$Nu_L = -128.3 + 0.3692 Ra_L^{1/4} + 64.7 \left(\frac{L}{D} \right) \quad (4.2)$$

For $AR = 1$

$$Nu_L = -0.1557 + 0.4718 Ra_L^{1/4} + 0.315 \left(\frac{L}{D} \right) \quad (4.3)$$

For $0.1 \leq AR \leq 0.2$

$$Nu_L = -0.3903 + 0.5399 Ra_L^{1/4} + 0.6367 \left(\frac{L}{D} \right) \quad (4.4)$$

Figures 4.1 – 4.9 show present results for both the adiabatic- and heated-top cases for varying Rayleigh numbers and aspect ratios. Furthermore, results using the technique of Eslami and Jafarpur are plotted(except for AR = 10 since that fell out of the range of applicability of the equations). Furthermore, the two experimental data points of Oosthuizen are plotted for AR = 1 and 2 in Figs. 4.5 and 4.6.

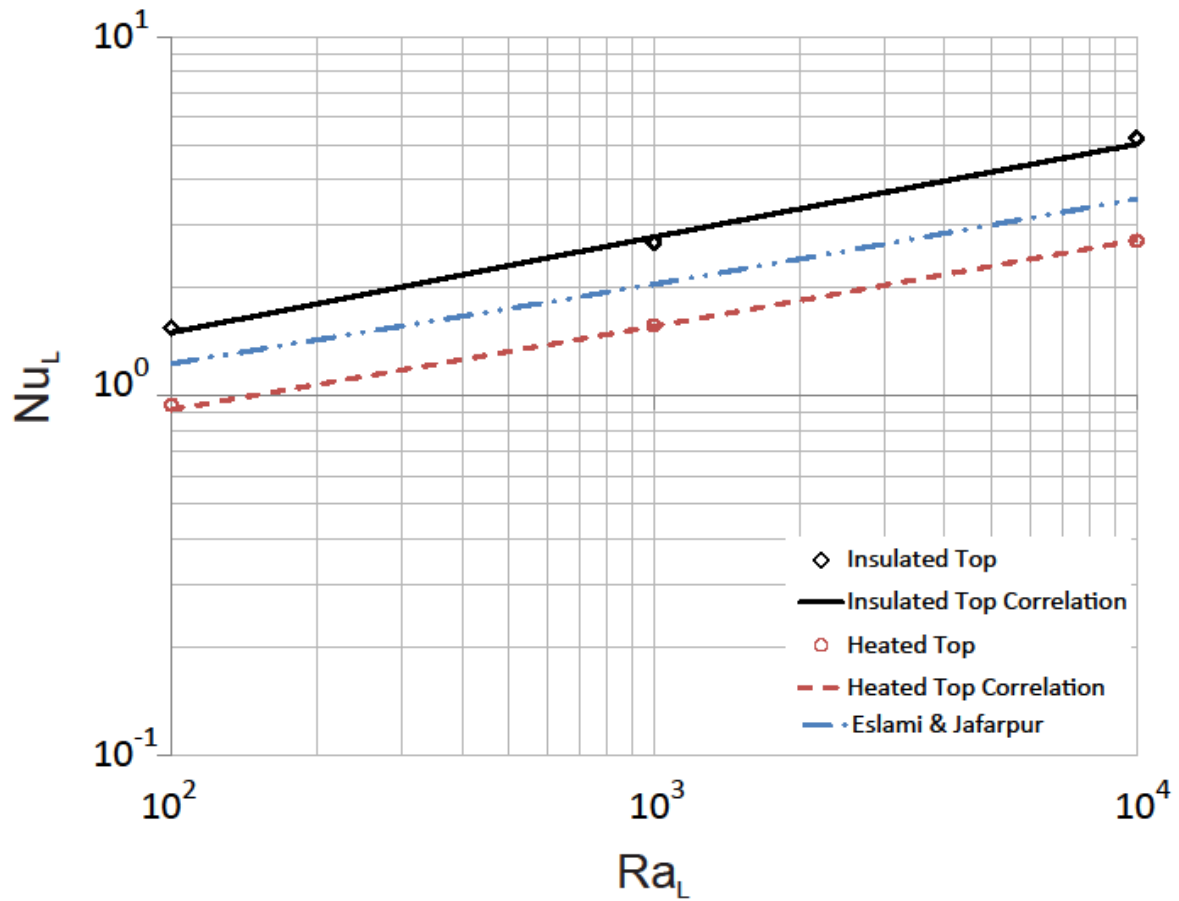


Fig. 4.1 Comparison of Average Nusselt Number versus Rayleigh Number for AR = 0.1.

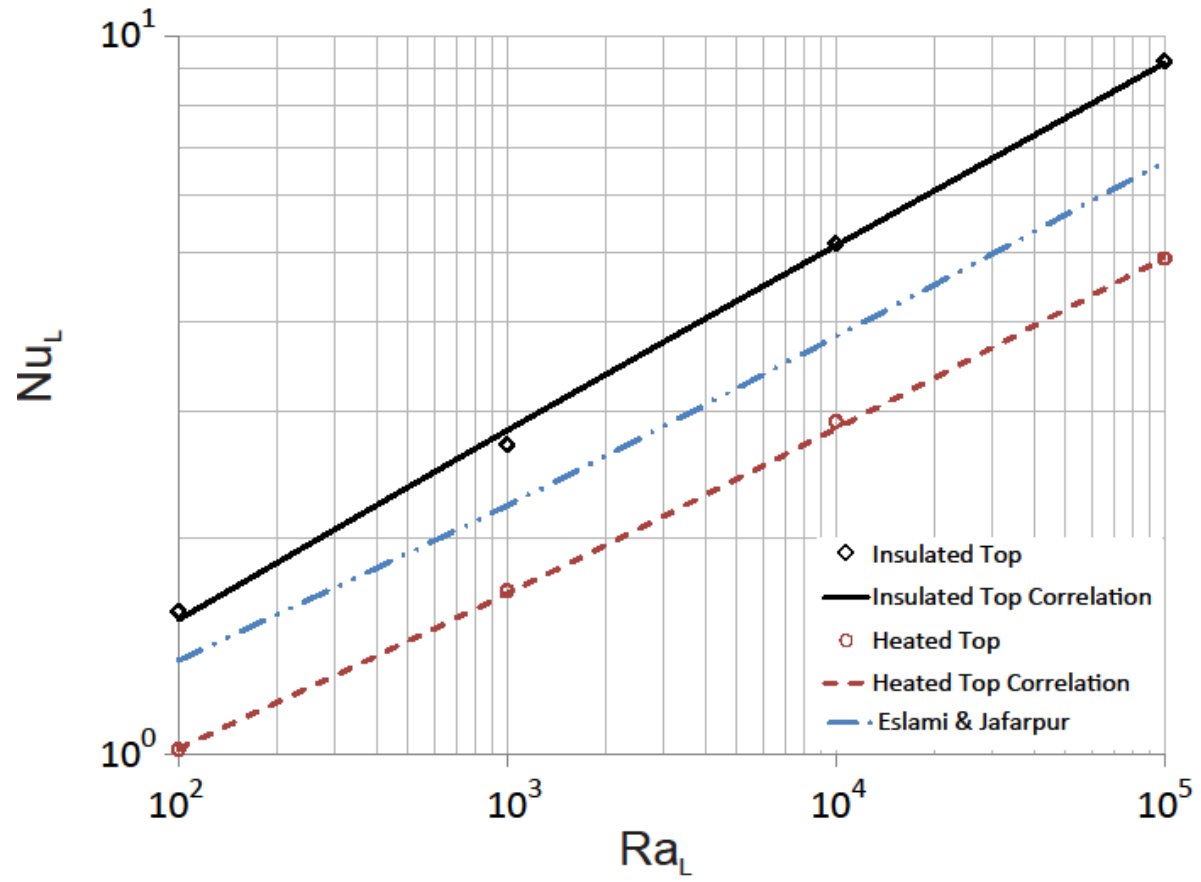


Fig. 4.2 Comparison of Average Nusselt Number versus Rayleigh Number for $AR = 0.125$.

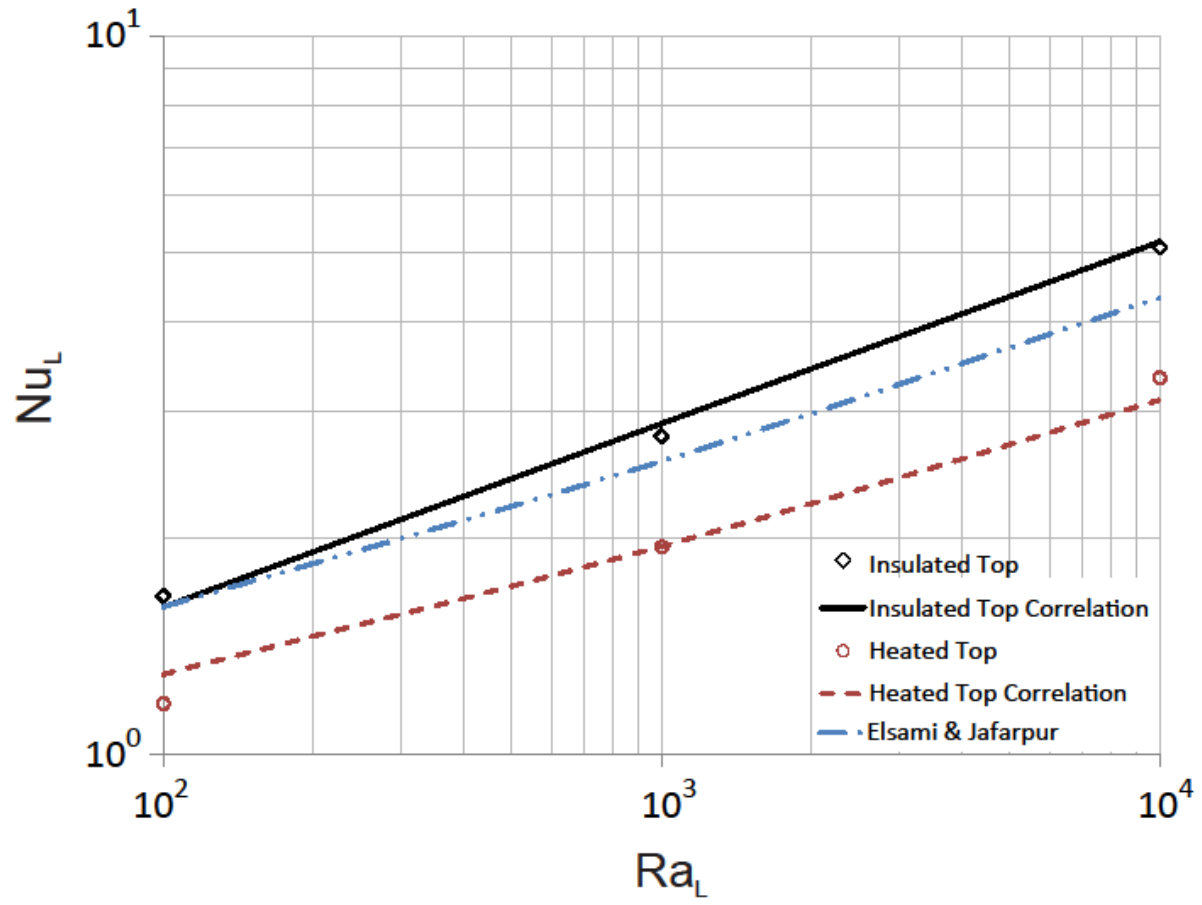


Fig. 4.3 Comparison of Average Nusselt Number versus Rayleigh Number for $AR = 0.2$.

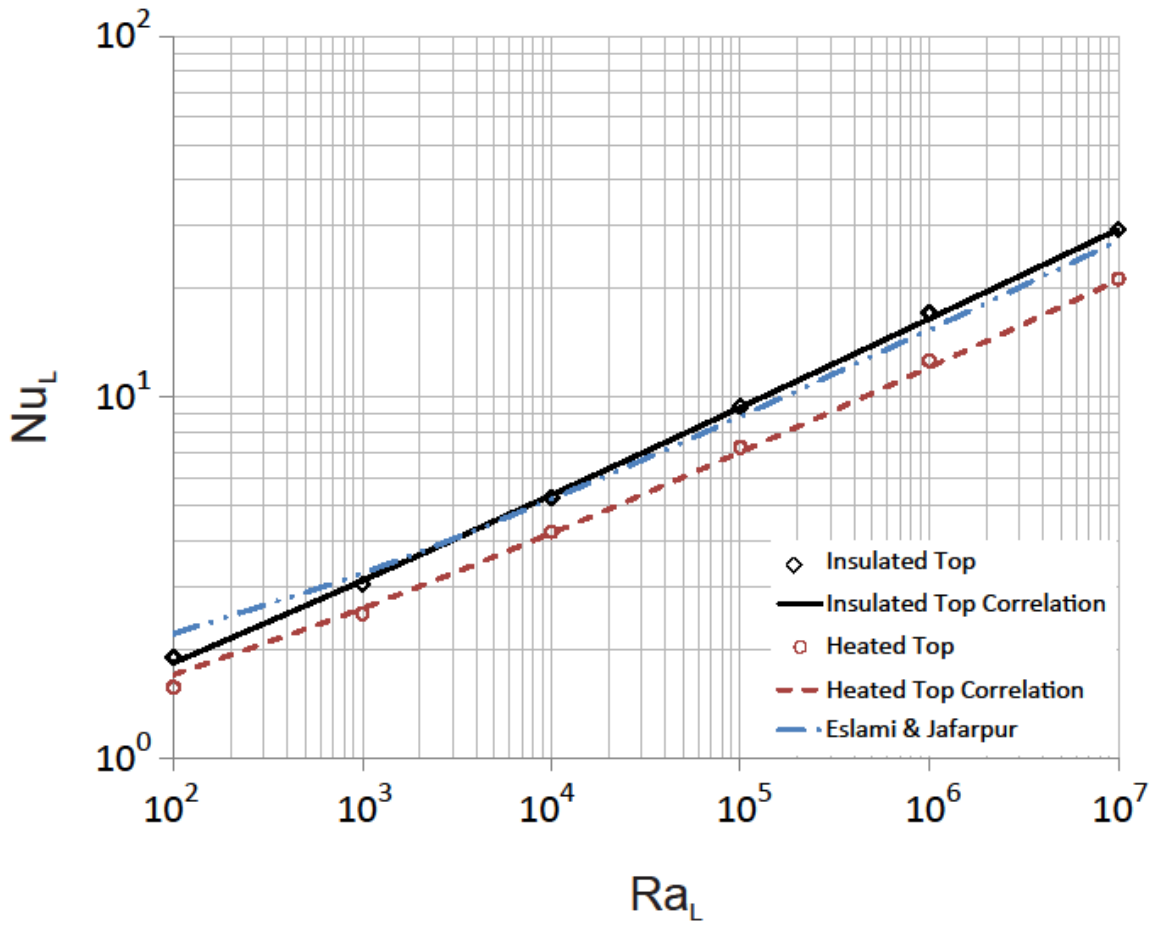


Fig. 4.4 Comparison of Average Nusselt Number versus Rayleigh Number for $AR = 0.5$.

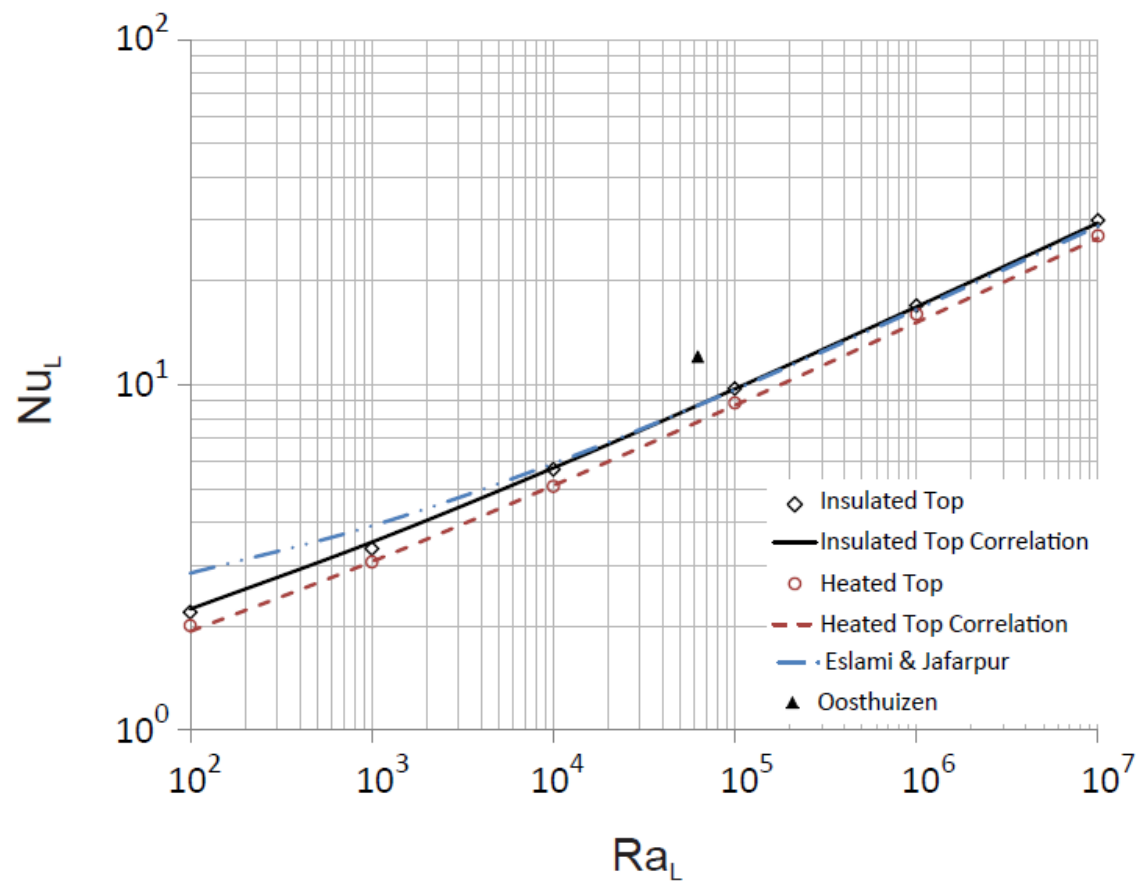


Fig. 4.5 Comparison of Average Nusselt Number versus Rayleigh Number for $AR = 1$.

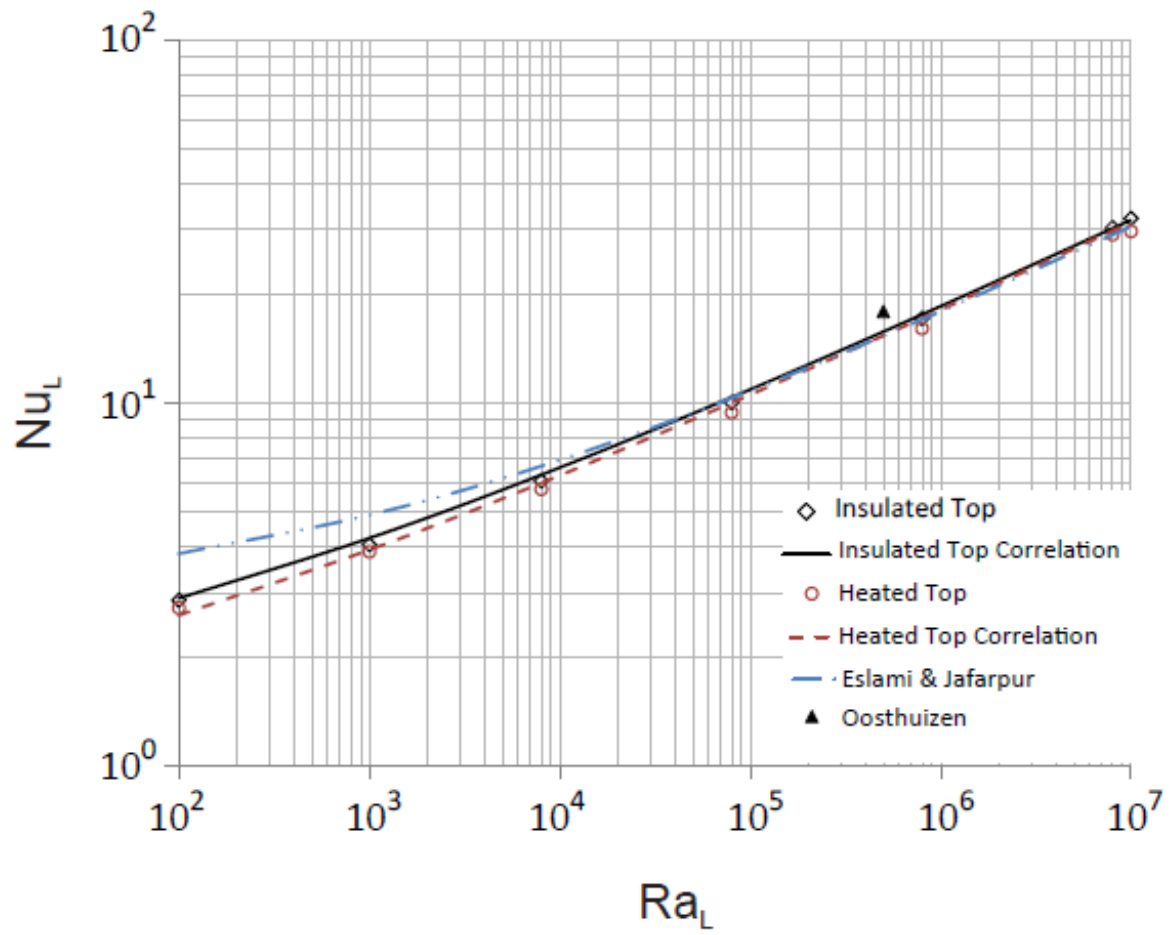


Fig. 4.6 Comparison of Average Nusselt Number versus Rayleigh Number for $AR = 2$.

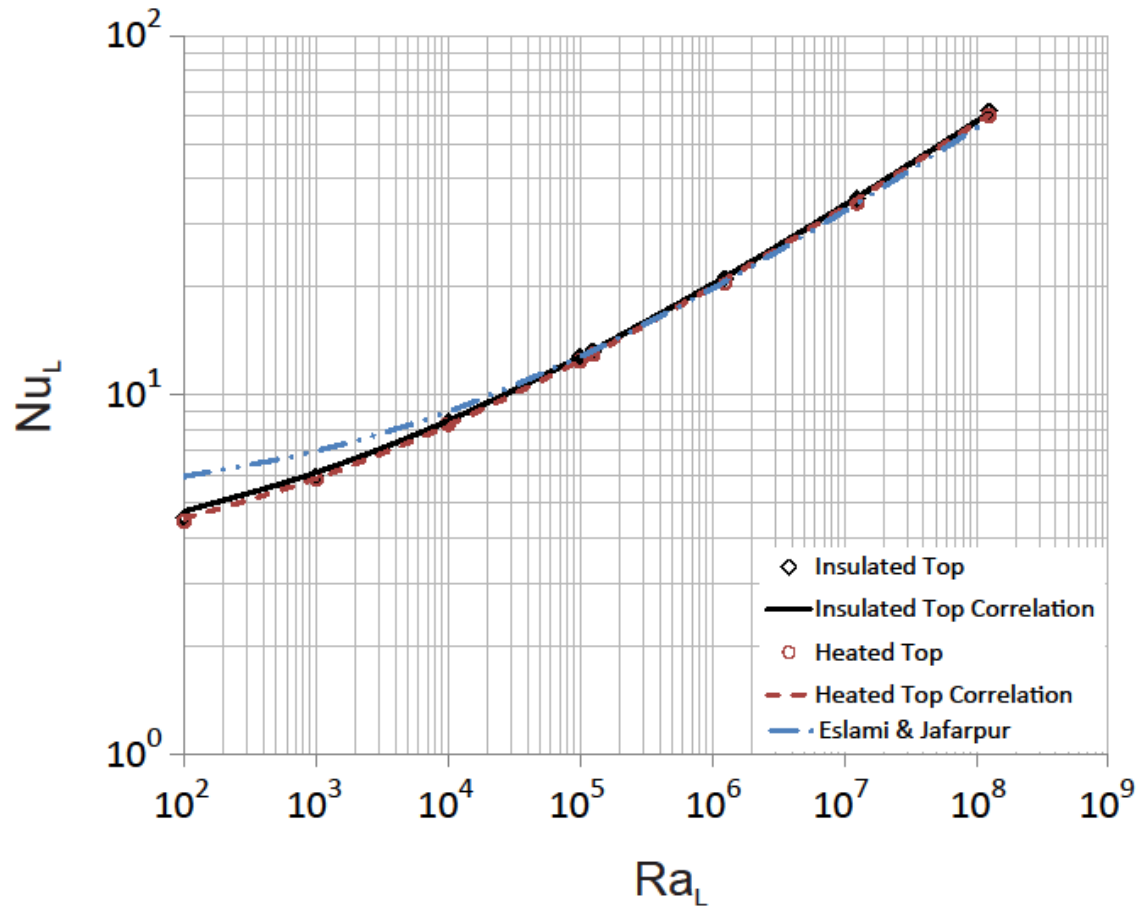


Fig. 4.7 Comparison of Average Nusselt Number versus Rayleigh Number for $AR = 5$.

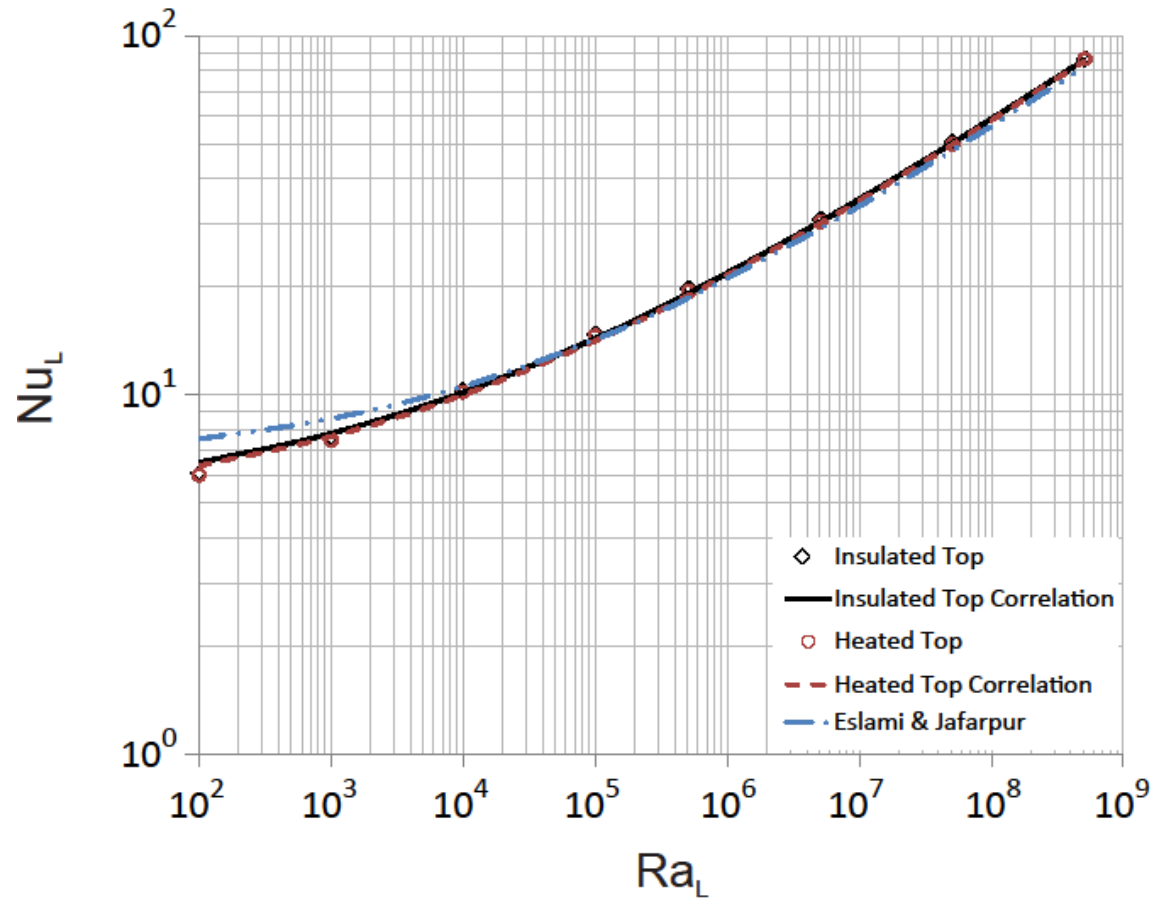


Fig. 4.8 Comparison of Average Nusselt Number versus Rayleigh Number for $AR = 8$.

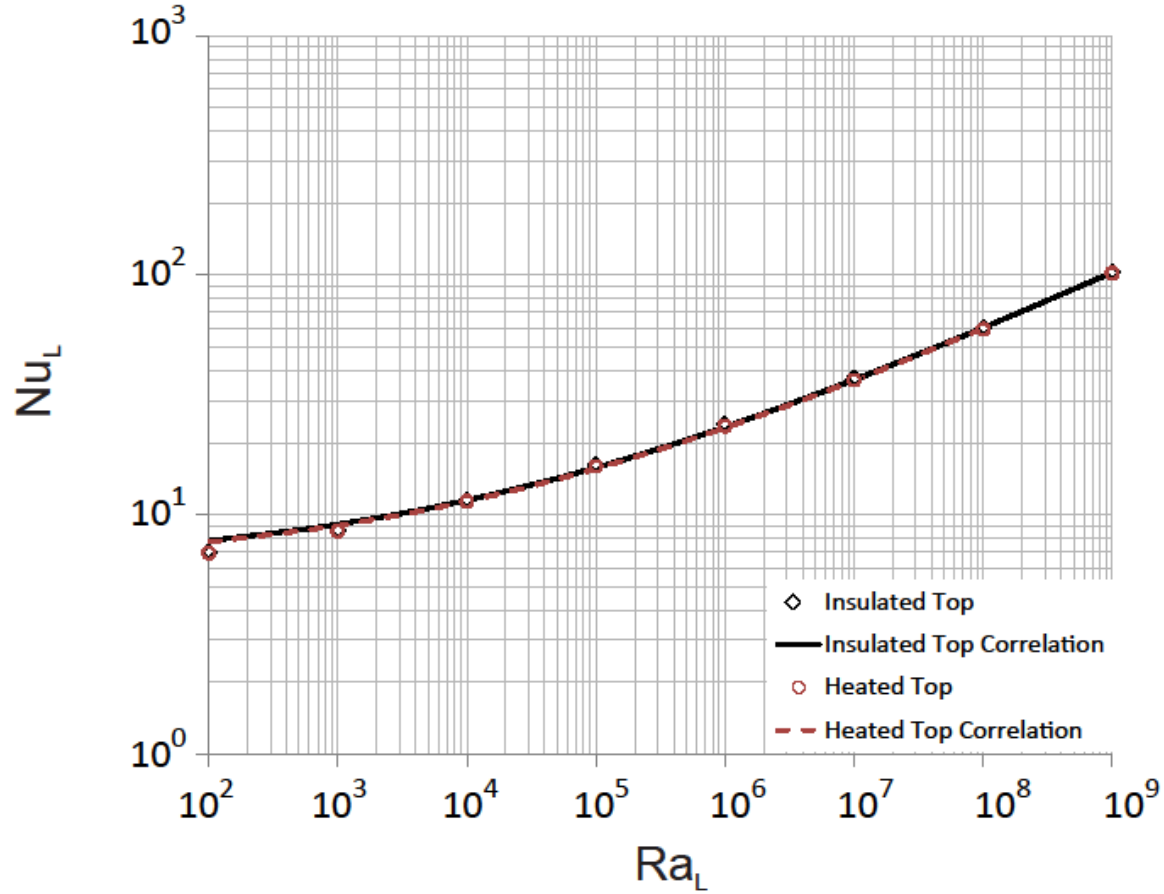


Fig. 4.9 Comparison of Average Nusselt Number versus Rayleigh Number for AR = 10.

Like Oosthuizen reported, the average Nusselt numbers for the heated top are lower than that for the adiabatic top. Solutions from Eslami and Jafarpur fell between the adiabatic- and heated-top cases for the lower aspect ratios ($AR \leq 0.2$) and lined up with the insulated-top case for $AR \geq 0.5$. The Eslami and Jafarpur solutions deviated at low values of the Rayleigh number, perhaps suggesting a Rayleigh-number limit for their solution. The Oosthuizen data points appear to be outliers on the graphs with an approximately 40% deviation for $AR = 1$ and 5% deviation for $AR = 2$.

The percent difference between the insulated-top case and the heated-top case remains relatively constant for all values of the Rayleigh numbers for a given aspect ratio, and as the aspect ratio increase, the percent difference decreases. For an $AR = 0.1$, the percent difference between the two is around 40%, for $AR = 1$, the difference is 10%, and for $AR = 10$, the percent difference is on the order of 1%. Nusselt numbers for heated-top cylinders with aspect ratios greater than 2 can be approximated using the adiabatic-top solution to within 5%.

CHAPTER 5

CONCLUSION

In the present study, numerical experiments have been performed to interrogate the average natural convection Nusselt numbers for laminar isothermal vertical cylinders situated on an adiabatic surface in a quiescent ambient environment for $Pr = 0.7$, $10^2 < Ra_L < 10^9$, and $0.1 < L/D < 10$. The case where the cylinder has an adiabatic top was compared to several other classical solutions, which are found in or referenced by commonly used heat transfer textbooks, as well as other solutions less cited. It was found that the classical solutions (Minkowycz and Sparrow, Cebeci) were not always in agreement with the present solution and other less-cited or referenced vertical cylinder solutions (LeFevre and Ede, Lee et al.). Furthermore, the limit for which the average Nusselt numbers for the flat-plate solution may be used as an approximation for the vertical cylinder (which, again, is referenced in all commonly used heat transfer textbooks) was, in some cases, too liberal, and in others, too conservative. A new average Nusselt number correlation was developed and a new guideline for Rayleigh-number limits for using the flat-plate approximation for each of the aspect ratios was discussed.

The case where the cylinder has a heated top has received less attention. Results from the present study show that the average Nusselt numbers for the heated top are less than that for the adiabatic top. Results are compared with known investigations (including a very recent study), but they are not in good agreement. Further analytical and experimental data is needed.

REFERENCES

- [1] Incropera, F. P., Dewitt, D. P., Bergman, T. L., and Lavine, A. S., 2007. Introduction to Heat Transfer 5th Ed. John Wiley & Sons, Inc., Hoboken, NJ.
- [2] Incropera, F. P., Dewitt, D. P., Bergman, T. L., and Lavine, A. S., 2007. Fundamentals of Heat and Mass Transfer 6th Ed. John Wiley & Sons, Inc., Hoboken, NJ.
- [3] Holman, J. P., 2010. Heat Transfer 10th Ed. Mc-Graw-Hill Companies, Inc., New York, NY.
- [4] Burmeister, L., 1993. Convective Heat Transfer 2nd Ed. John Wiley & Sons, Inc., New York, NY.
- [5] Gebhart, B., Jaluria, Y., Mahajan, R. L., and Sammakia, B., 1988. Buoyancy Induced Flows and Transport: Reference Edition. Hemisphere Publishing Company, New York, NY.
- [6] Sparrow, E. M., and Gregg, J. L., 1956. "Laminar-free-convection heat transfer from the outer surface of a vertical circular cylinder". Transactions of the ASME, 78, pp. 1823–1829.
- [7] LeFevre, E. J., and Ede, A. J., 1956. "Laminar free convection from the outer surface of a vertical cylinder". In Proceedings of the 9th International Congress on Applied Mechanics, pp. 175–183.
- [8] Ede, A. J., 1967. Advances in Heat Transfer. ch. Advances in Free Convection, pp. 1–64.
- [9] Cebeci, T., 1974. "Laminar-free-convective-heat transfer from the outer surface of a vertical circular cylinder". In Proceedings of the 5th International Heat Transfer Conference, Tokyo, pp. 1–64.
- [10] Popiel, C. O., 2008. "Free convection heat transfer from vertical slender cylinders: A review". Heat Transfer Engineering, 29, pp. 521–536.
- [11] Churchill, S. W., and Chu, H. H. S., 1975. "Correlating equations for laminar and turbulent free convection from a vertical plate". International Journal of Heat and Mass Transfer, 18, pp. 1323–1329.
- [12] Minkowycz, W. J., and Sparrow, E. M., 1974. "Local non similar solutions for natural convection on a vertical cylinder". Journal of Heat Transfer, 96, pp. 178–183.
- [13] Lee, H. R., Chen, T. S., and Armaly, B. F., 1988. "Natural convection along slender vertical cylinders with variable surface temperature". Journal of Heat Transfer, 110, pp. 103–108.

- [14] Fujii, T., and Uehara, H., 1970. "Laminar natural-convective heat transfer from the outside of a vertical cylinder". *International Journal of Heat and Mass Transfer*, 13, pp. 607–615.
- [15] Munoz-Cobo, J. L., Cover'an, J. M., and Chiva, S., 2003. "Explicit formulas for laminar natural convection heat transfer along vertical cylinders with power-law wall temperature distributions". *Heat and Mass Transfer*, 39, pp. 215–222.
- [16] Kimura, F., Tachibana, T., Kitamura, K., and Hosokawa, T., 2004. "Fluid flow and heat transfer of natural convection around heated vertical cylinders (effect of cylinder diameter)". *JSME International Journal Series B*, 47, pp. 159–161.
- [17] Popiel, C. O., Wojtkowiak, J., and Bober, K., 2007. "Laminar free convective heat transfer from isothermal vertical slender cylinders". *Experimental Thermal and Fluid Science*, 32, pp. 607–613.
- [18] Gori, F., Serrano, M. G., and Wang, Y., 2006. "Natural convection along a vertical thin cylinder with uniform and constant wall heat flux". *International Journal of Thermophysics*, 27, pp. 1527–1538.
- [19] Oosthuizen, P. H., 5. "Free convective heat transfer from vertical cylinders with exposed ends". *Transactions of the Canadian Society for Mechanical Engineering*, 1978-1979, pp. 231–234.
- [20] Eslami, M., and Jafarpur, K., 2011. "Laminar natural convection heat transfer from isothermal vertical cylinders with active ends". *Heat Transfer Engineering*, 32, pp. 506–513.
- [21] Yovanovich, M. M., 1987. "On the effect of shape, aspect ratio and orientation upon natural convection from isothermal bodies of complex shape". *ASME HTD*, 82, pp. 121–129.
- [22] Lee, S., Yovanovich, M. M., and Jafarpur, K., 1991. "Effects of geometry and orientation on laminar natural convection from isothermal bodies". *Journal of Thermophysics and Heat Transfer*, 5, pp. 2208–216.
- [23] Churchill, S., and Churchill, R., 1975. "A comprehensive correlating equation for heat and component transfer by free convection". *AIChE Journal*, 21, pp. 604–606.
- [24] Yovanovich, M., 1987. "New nusselt and sherwood numbers for arbitrary isopotential geometries at near zero pecletand rayleigh numbers". In *Proceedings of the 22nd Thermophysics Conference*, AIAA, Honolulu, HI, USA.
- [25] Zanotti, C., P. Giuliani, S. Arnaboldi, and A. Tuissi, 2011. " Analysis of wire position and operating conditions on Functioning of NiTi Wires for Shape Memory Actuators". *Journal of Materials Engineering and Performance*, 20, pp. 688-696.